

IGNITION TRANSIENTS OF A GASEOUS CH₄/O₂ COAXIAL JET

J. Sender, C. Manfretti, M. Oswald, C. Pauly

Deutsches Zentrum für Luft- und Raumfahrt
Raumfahrtantriebe
74239 Hardthausen, Deutschland

ABSTRACT

Several experimental investigations of the ignition transient for liquid propellant rocket engines using H₂/LOX have already been performed at the M3 test facility of DLR Lampoldshausen. To better understand the ignition and stability also of hydrocarbon/LOX driven engines new tests on the ignition of a gaseous O₂ / CH₄ coaxial jet for a range of nondimensional injection parameters, such as J , V_{ratio} and p_{cc} , were done. A combustion chamber (CC) with large lateral windows and small windows on both the top and bottom sides, equipped with a single coaxial injector, was used. Ignition was achieved by induced plasma break-down of a laser pulse focused downstream the injector. The ignition and stabilisation phase was visualized using Schlieren technique and recording of spontaneous fluorescence of intermediate existing OH radicals by high speed videography. Several phases during ignition have been found with specific phenomenology and which are dependent on parameters such as the ignition delay or mass fluxes of injected media. The pressure peak observed and its delay appears to be highly influenced by the injected masses of fuel and/or oxidizer before ignition. The CC pressure during steady state is an influent parameter to stabilize the flame near the injector. Flame lifting is observed to depend also on the velocity ratio of oxidizer and fuel, i.e. the mixing of both.

disadvantages are minimised when methane is implemented [5].

Results related to ignition and combustion of methane and oxygen from the GCHO campaign are presented. The campaign was conceived so as to focus on ignition and flame stabilisation processes whilst at the same time providing detailed data to support numerical simulations of the injection, ignition, and combustion processes.

The campaign implemented a gaseous O₂/CH₄ coaxial jet, to better understand the ignition and stability of hydrocarbon/LOX driven engines for a range of non-dimensional injection parameters, such as J , V_{ratio} and p_{cc} .

EXPERIMENTAL SET-UP

Combustion chamber

The GCHO campaign made use of the M3 Micro-combustor whose two most important features are the wide optical quartz windows which provide a complete optical access to the combustion chamber and the small windows located in the upper part of the chamber are used to allow the access of the converged laser beam to the chamber. The Micro-combustor is a horizontally mounted combustion chamber (CC). The section of the combustion chamber is rectangular with dimensions: 60 x 60 x 140 mm.

INTRODUCTION

Ignition is one of the most important phases during the start-up transients of a liquid rocket engine and has led to failures in past launches (Ariane flights V15 and V18, involving the upper stage cryogenic HM7B engine). For upper stage engines, such as the European VINCI and Aestus engine, re-ignition is also of particular interest due to the multiple payload capability of the Ariane 5 launcher. Clearly for central and upper stage engine, ignition occurs under widely different conditions both in terms of pressure and temperature. These have an important impact on the atomisation of the propellants as various studies have shown. Several studies have been performed addressing transient ignition phenomena [7], [8],[9]. Amongst other objectives, these studies aimed at examining the spray behaviour of oxygen when combined to both H₂ and CH₄ in an attempt to investigate into potential differences between the two propellant couples spurred by an growing interest which alternative, so called "green", propellants have seen. Although the propellant couple H₂/O₂ is the most energetic, providing the highest Isp values, due to the low molecular weight of H₂, many difficulties are encountered in their implementation. The best performing non-toxic alternatives to H₂ belong to the family of hydrocarbons, i.e. methane, propane and kerosene, and present several advantages like higher density or easier storability at ambient conditions (lower cooling efforts). Known disadvantages are their known tendency to produce soot reducing the ISP and a carbon layer at the cooling channel wall, which lowers the cooling efficiency. These

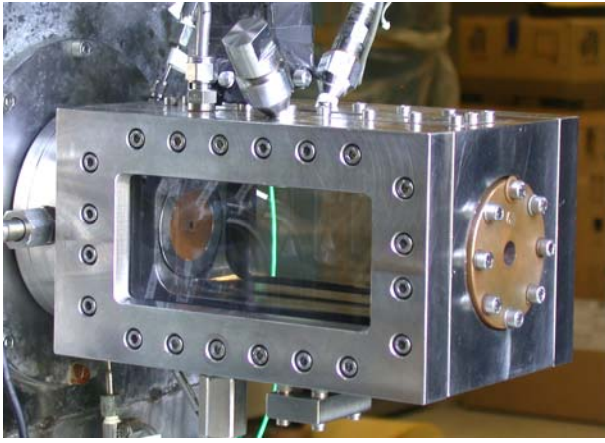


Figure 1: M3.1 Combustion Chamber

The combustion chamber design allows the installation of a multitude of different injector elements. In this case use was made of a single coaxial injector with no recess or tapering. Varying of the co-axial element diameters is possible, allowing flexibility in terms of injection conditions which can be achieved. Additional geometric variations can be made in both the exit nozzle, in order to fix the total mass flow rate, and in the sonic nozzle used to determine the mass flow rate of the gaseous propellants.

Figure 2 depicts the injector head implemented

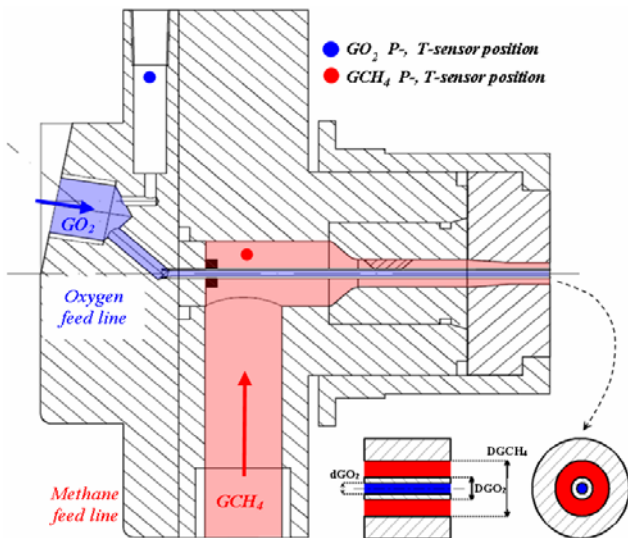


Figure 2: Methane/Oxygen Injector Dome Geometry

Laser ignition

Numerical simulation of the ignition processes plays a fundamental role in the attempt of obtaining a better understanding of the phenomena at work. Numerical simulations are however seriously limited due to the great detail required for the simulation boundary conditions. This is one of the reasons which makes laser ignition an attractive alternative to the conventional torch ignition used. Furthermore, although laser ignition is less representative of the conventional ignition methods currently implemented, it provides precise boundary conditions both in terms of spatial positioning of the ignition location as well as in the exact time of ignition. The data recording of both the optical diagnostics and sensors can be synchronised with the igniting laser pulse (precision of +/- 10 μ s).

For these reasons laser ignition has been widely applied at the M3.1 test bench and was implemented in the GCHO campaign.

The ignition system is provided by an Nd-YAG Laser at 532 nm. The laser beam, with an energy of ca. 150mJ per pulse and a pulse length of 10 ns, is focused inside the chamber thus generating an induced plasma directly in the flow (see Figure 3). The minimum breakdown energy deposition is for a methane/air mixture of 4 mJ [11].

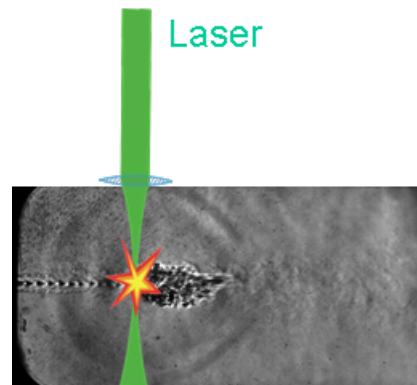


Figure 3: Laser Beam Focused Inside the Chamber

The ignition location was set to 31 mm downstream of the injector plate and 1 mm off jet axis. The approximated size of the induced plasma has been determined, by implementing OH and Schlieren images, to be: $dX_{\text{plasma}} = 2.25 \text{ mm} \pm 0.25 \text{ mm}$ $dY_{\text{plasma}} = 3.4 \text{ mm} \pm 0.4 \text{ mm}$. A more in-depth description of the laser triggering method adopted is given in [2]

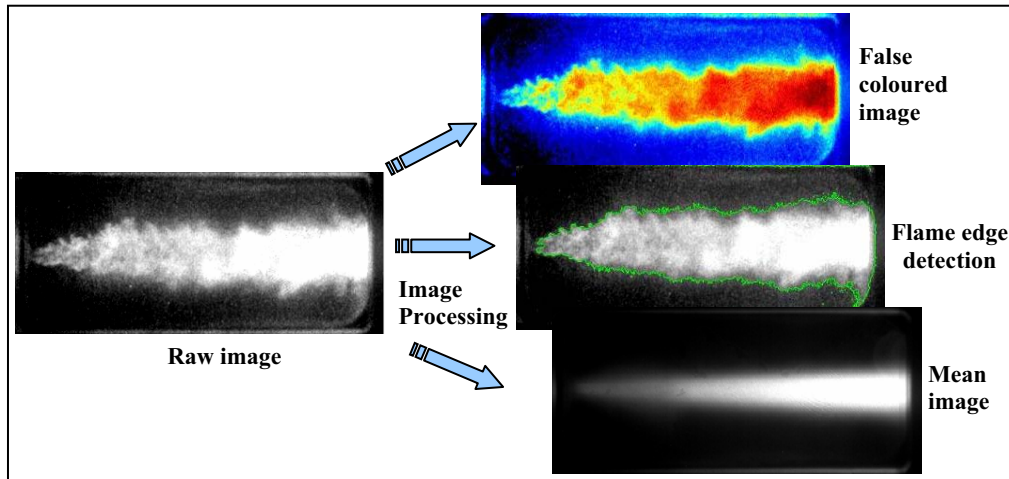


Figure 4: Image Processing Performed on OH Images

Optical diagnostic systems

The campaign relied on two different optical diagnostic systems: Schlieren and OH imaging.

Schlieren

A standard Z-Schlieren set-up with two different zoom settings was used. A high speed CCD video camera at 2000 fps and with a resolution of 512 x 256 pixel was implemented for image recording purposes. For better resolution of the near-injector exit field (40 mm x 80 mm), zooming was performed for test cases A and B. Images for test case C and D were recorded using a lower magnification resulting in a window size of 60 mm x 110 mm. An example of the latter can be seen in Figure 3.

OH imaging

During combustion of hydrocarbon intermittently OH radicals are present which, if excited, emit light at 305 nm. Excitation caused by combustion-related heat release results in spontaneous emission. This spontaneous emission in the UV-range was recorded by an intensified high speed CCD video camera. The complete combustion chamber is visualized with a resolution of 512 x 256 pixels and a frame rate of 12500 fps. A band-pass filter (310 nm \pm 5 nm) is used to select only the emission of the OH-radical.

The recorded OH emission images have been post-processed using image processing tools. A false colorization of the black and white images was applied in order to get a better visualization of the intensity gradient. By using a threshold value on the grey levels of the image, detection of the flame front is possible. Calculated average images during steady combustion are used to determine the final lift-off distance of the flame. Figure 4 illustrates the image processing steps.

Test time sequence

Different time sequences were implemented throughout the campaign. Common features include a continuous purging of the combustion chamber prior to priming and ignition such that the chamber can be considered to be completely filled with nitrogen at commencing of the test startup sequence. The fuel valve is opened prior to opening of the oxidiser valve to ensure a fuel-rich mixture within the chamber at ignition. Hot flow testing was performed for one second at steady-state conditions, approximately 80 ms and 50 ms of flow transients were observed for methane and oxygen respectively.

Test conditions

Four different configurations, with varying geometry, each corresponding to a test case, were tested in the GCHO campaign.

Test case A with an oxygen injector diameter of 1.6 mm

Table 1 Testing Conditions for Test Cases A-D

| Test Case | u_{CH_4} | u_{O_2} | \dot{m}_{tot} | Pcc | J | V_{Ratio} |
|-----------|------------|-----------|-----------------|-----------|-------------------|---------------|
| | [m/s] | [m/s] | [g/s] | [bar] | [-] | [-] |
| A | 133 | 304 | 3.1 | 1.5 | 0.03 | 0.44 |
| B | 212-359 | 298 | 3.1 – 5.9 | 1.5 – 3.6 | 0.14 - 0.21 | 0.71- 1.18 |
| C1 | 424 | 305 | 4.6 | 2.3 | 1.06 | 1.39 |
| C2 | 351 | 201 | 2.1 | 2.3 | 1.56 | 1.74 |
| D | 368 | 302 | 4.6 | 2.3 | 0.37 | 1.22 |

was chosen for comparison with a precedent test case with GH_2/GOX . However during the test, no attached flame was observed with this configuration.

Test cases B through D have been set up with an enlarged diameter to enable a wider range of available oxygen injection velocities.

In test case C (C1 & C2) the influence of the injection velocity was studied in more detail using two different combustion chamber nozzles, 4 mm and 6 mm diameter respectively. The resulting injection conditions are given in Table 1.

IGNITION PHENOMENOLOGY OF A GOX/GCH4 COAXIAL JET (GCHO CAMPAIGN)

General remarks

Based on the evaluation of the OH and Schlieren images, the existence of three different ignition scenarios has been observed.

A non reliable ignition where the flame is blown out and extinguished has been found and two successful other ignition types: one with smooth evolution of the flame front and of the chamber pressure, the other one with much stronger transient phenomenology. Additional observations include three different transient phases characterising the evolution of the flame front for each of the reliable ignition scenarios. These three phases are, in order of appearance: a blow down phase, where the flame is blown downstream (or even extinguishes); an expansion phase, where the flame increases in size and intensity; and finally a stabilization phase, where the flame stabilizes and is either detached or attached to the injector. The duration of each phase depends on the combination of fluid injection conditions and injector geometry. Typically, the blow down phase lasted between 0.5 and 1.5 ms and the expansion phase between 6 and 17 ms.

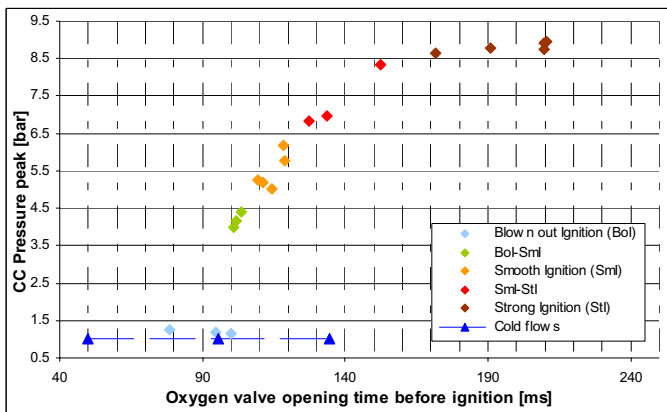


Figure 5 Ignition Scenario Dependency on Ignition Delay

An important parameter determining to what extent each phase is present and thus determining which ignition scenario occurs is the time delay between opening of the propellant valves and the laser pulse (“ignition delay”).

Figure 5 illustrates this phenomenon giving the ignition peak pressures for tests performed with different ignition delays (test case A). Optimal setting of this delay results in reliable ignition but with differences in the expansion phase. Extending the delay increases the mass of unburnt gases in the

chamber resulting in higher pressure peaks at ignition, leading, in extreme cases, to a direct and significant expansion of the flame without relevant blow down of the initial flame kernel (strong ignition, see Figure 8). If however the delay is reduced only the first ignition phase (blow down phase) is observed and the flame extinguishes.

Blown out scenario

In this scenario the flame kernel is blown down towards the exit nozzle just after ignition and extinguishes. Due to the small ignition delay there is an insufficient amount of

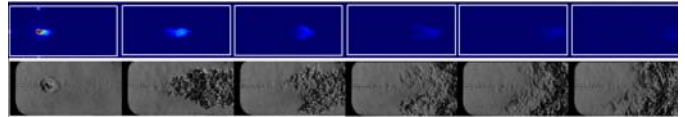


Figure 6: OH and Schlieren Images of Blown Out Scenario (0 to ~7.5 ms)

propellants within the chamber to sustain combustion. Figure 6 depicts such a blown out ignition, where the images are displayed for time intervals of 1.44 ms and 1.5 ms for OH (top) and Schlieren (bottom) imaging respectively (the flow direction is left to right). The first Schlieren images show a blast wave of the plasma breakdown caused by the focused laser beam. At the exit of the oxygen injector crisscrossed shocks structures are visible, characteristic of an under-expanded jet and confirming the sonic condition of the oxygen jet at ignition.

Smooth and strong ignition scenarios

During the blow down phase hot gas expands, depending on the accumulated amount of reactants before ignition, more or less rapidly. For reliable ignition cases, this expansion passes over into the so-called expansion phase. The hot gases expand both in the upstream and downstream directions. The hot gases moving in the downstream direction are redirected in the recirculation zone at the combustor exit, re-circulate and realign along the central propellant jet. The interaction of these hot gases with the unburnt and colder propellants leads to an efficient local mixing allowing the propagation of the flame towards the injector. In this case the flame front velocity is high enough (in comparison to the propellants injection velocity) to allow the attachment of the flame at the injector lips. Figure 7 depicts such a smooth ignition, where the images are displayed for time intervals of 0.44ms and 0.5 ms for OH (top) and Schlieren (bottom) imaging respectively.

In case of a longer delay between valve opening and ignition the sudden consumption of all accumulated propellants induces a high chamber pressure peak, i.e. a strong ignition. The exhaust of propellants is choked and a backflow of gases from the chamber into the injector dome occurs. This phenomenon is observed thanks to the dome pressure readings. This is also supported by an analysis of OH emission images (see Figure 8) where after 4 ms the flame extinguishes at injector lips, detaches from the injector plate and is blown out. After a certain delay (at around 6ms), a re-ignition is observed in proximity of the injector exhaust.

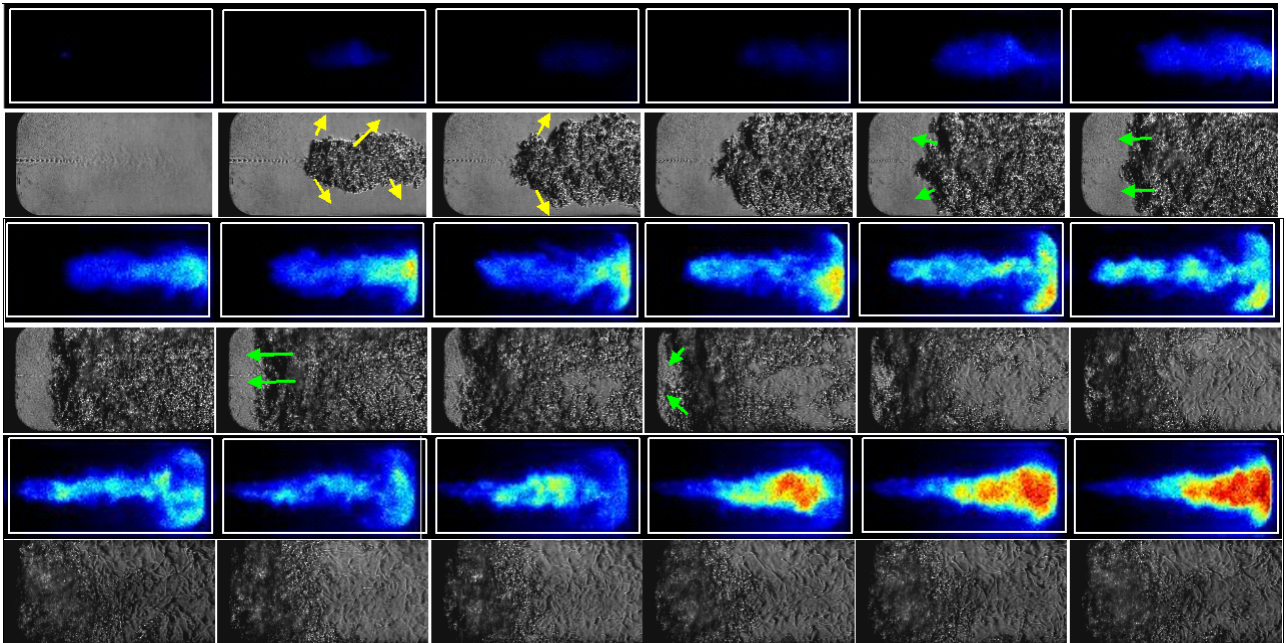


Figure 7: OH and Schlieren Images of a Smooth Ignition Scenario (0 to ~8.5 ms)

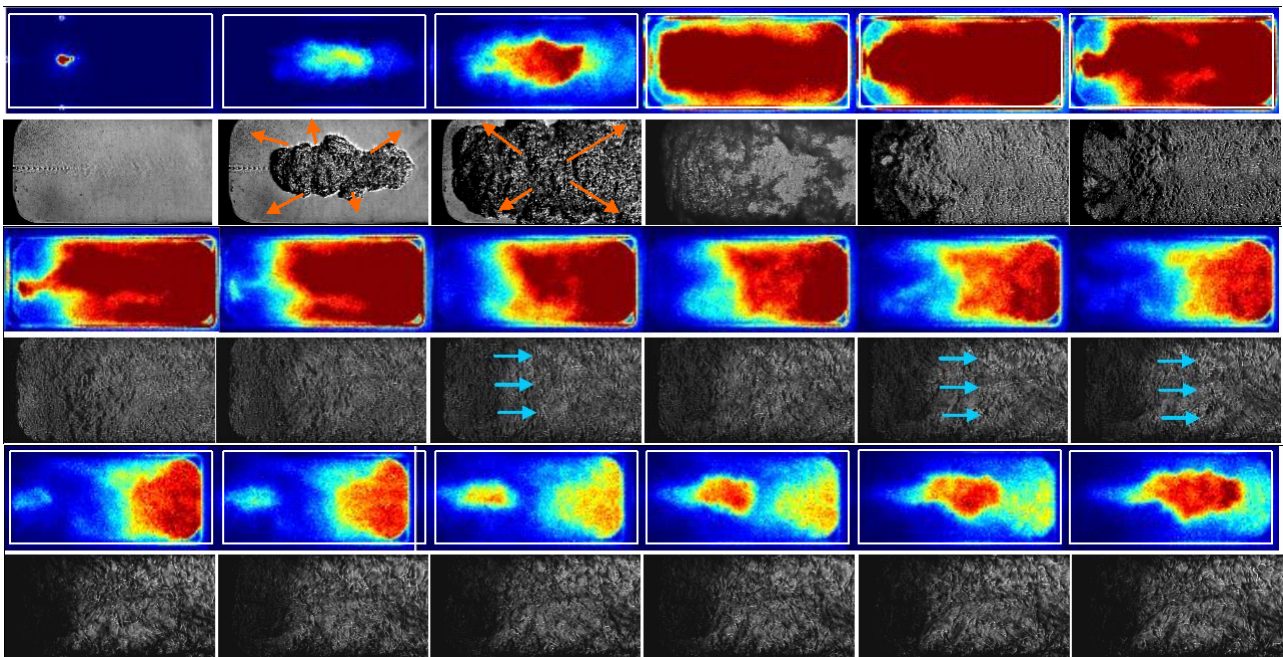


Figure 8: OH and Schlieren Images of a Strong Ignition Scenario (0 to ~8.5 ms)

Influence of propellant injection velocity

Two test cases (C1 and C2) have been defined to investigate the role of the propellant injection velocity on the ignition phenomenology. Injector dimensions, mixture ratio, momentum flux and velocity ratio, and combustion chamber pressure were identical for steady state combustion in both test cases. Changing of the nozzle diameter results in higher injection velocities in case C1 compared to case C2 (correspondingly is the mass flow also higher, see Table 1).

Having established that the ignition delay plays a critical role in the ignition behaviour, adequate delays were chosen to result in similar amounts of unburnt gas in the chamber prior to ignition. Consequently, both test cases show smooth ignition behaviour and the effect of injection velocity can be investigated.

For both test cases the flame evolution during the ignition transient is tracked by determining the position of the upstream flame front (distance to the injector plate) from OH emission images. The data are shown in Figure 9. The different ignition phases discussed above are clearly visible. However there are particular differences between both cases.

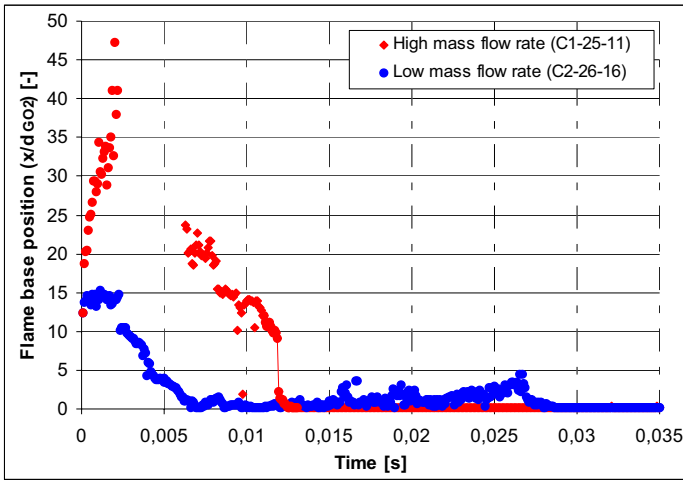


Figure 9: Flame Base Position for Attached Flames with Different Mass Fluxes

For the higher injection velocity case C1 the flame is blown down to a large distance from the injector plate. The flame intensity is strongly decreasing and rather no more visible, for that reason between 2ms and 6ms the flame front could not be tracked. When the flame expands into upstream direction during the expansion phase chemiluminescence recovers at a position several diameters downstream the injector. From there the flame base moves slowly towards the injector and finally anchors there. The phenomenon of very low chemiluminescence intensity has also been observed in former investigations especially with CH_4/LOX ([10]).

In the lower injection velocity case C2 the upstream flame front is not blown down and starts after 2ms to move upstream. For both test cases the upstream flame front movement is found to have similar velocity although the propellant velocities are much higher in case C1 as compared to C2. Attachment occurs at around 6 ms for case C2, earlier than the 12.5 ms required in the higher mass flow case C1. Once anchored, the flames stayed stabilized at the injector during the rest of the steady combustion for both cases.

Flame stabilization

Figure 10 shows flame images of the stabilization phase, i.e. the period between the end of the flame expansion and the final steady state combustion for all injection conditions (A, B, C1, C2 and D). The images have been averaged during the time period between 40 and 120 ms after ignition, they are aligned with decreasing lift off distance.

It can be clearly seen that for low values of velocity ratio and J number, the flame stays at a significant distance from the injector lips (more than 15 times the inner oxygen injector diameter). Above a critical value of the momentum flux ratio J or velocity ratio the flame becomes stable and stays attached at the injector lips. The shape of the flame depends whether it is attached or detached. Detached flames exhibit a parabolic like shape with the maximum intensity localized at the head of the flame. With increasing J the distance of the flame head moves upstream and its shape changes to a divergent cone, when it is attached to the injector. For the attached flame the maximum flame emission moves upstream with increasing

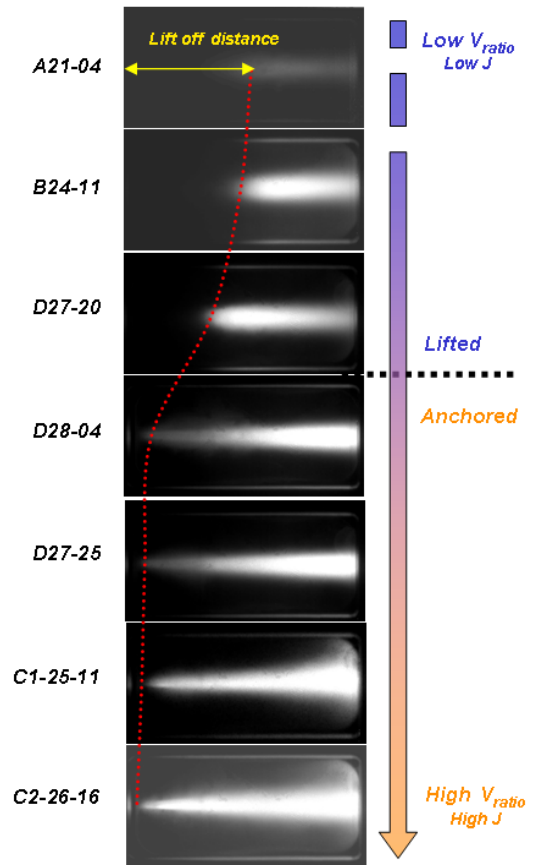


Figure 10: Lifted and Anchored Flames

momentum flux ratio and the flame angle is increasing too. Figure 11 shows this correlation more clearly, in giving all tests performed in a J- V_{ratio} plot. Critical values of 0.29 and 0.8 for J and V_{ratio} respectively appear to separate the two flame stabilization regions observed during this test campaign.

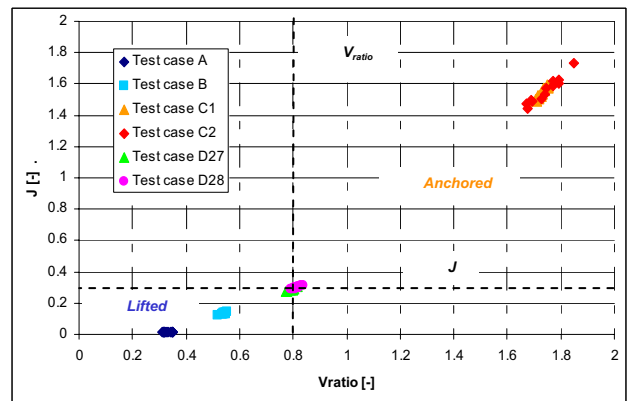


Figure 11: Tests with Stable and Lifted Flame

For detached flames (case B) the tests show a dependency of the lift-off distance on the chamber pressure for steady state conditions. Increasing the chamber pressure results in a reduction of the lift-off distance and favours the attachment of the flame. The flame lift-off distance as a function of chamber pressure is shown in Figure 12, the lift-off distance x/d_{O_2} decreases from 30 to less than 15 when increasing PCC from 1.5 to 3 bar pressure.

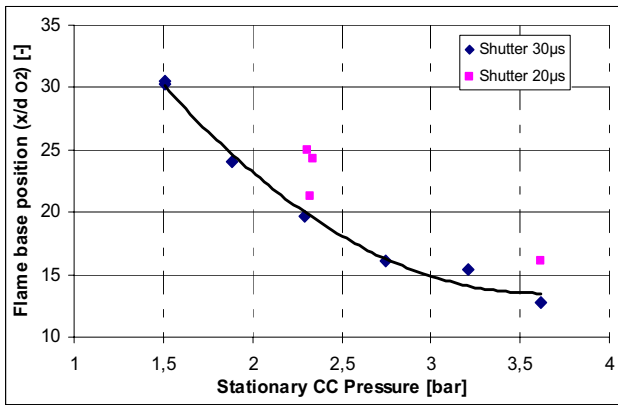


Figure 12: Lift off Distance for Different P_c

SUMMARY AND CONCLUSIONS

The transient process following laser induced ignition of a coaxial CH_4/O_2 -jet has been found to follow different scenarios of specific phenomenology: flame blown out, smooth, and strong ignition. Which scenario is realized is strongly controlled by the ignition delay. The amount of unburnt gas in the combustor at the time of ignition has a major influence on the ignition transient.

Increasing the mass flow rate is resulting in a prolongation of the time to stabilize the flame. The flame is convected downstream at a longer distance by the higher injection velocities in this case before it moves upstream again due to the expansion of the flame kernel.

Momentum flux and velocity ratio has been shown to control whether the flame is stabilized in an attached or detached mode. Increasing the fuel-to-oxidizer momentum flux ratio favours the attachment of the stabilized flame. Below a critical momentum flux ratio the flame becomes detached. The importance of this parameter has also been quoted by other groups for gaseous methane and oxygen injection [6].

Increasing the steady state chamber pressure is reducing the lift-off distance for detached flames. Previous studies have shown that for higher chamber pressures methane/oxygen flames stabilize attached to the injector ([3], [5]). For lower pressures the anchoring of the methane flame seems to be much more dependant on injection parameters (see also [2], [3], [6]).

NOMENCLATURE

| Symbol | Quantity | SI Unit |
|---------------------------------|--|---------|
| CC | combustion chamber | n.a. |
| d, D | inner diameter, outer diameter | mm |
| fps | frame per second | 1/s |
| GO_2 , GO_2 | gaseous oxygen | n.a. |
| GCH_4 , GCH_4 | gaseous methane | n.a. |
| J | momentum flux ratio, $J = (\rho u^2)_{\text{CH}_4} / (\rho u^2)_{\text{O}_2}$ | - |
| \dot{m} | mass flow rate | g/s |
| p, P | pressure | Pa |

| | | |
|-------------|---|-----------------|
| R_{of} | mixture ratio, $R_{of} = \dot{m}_{\text{O}_2} / \dot{m}_{\text{CH}_4}$ | - |
| T | temperature | K |
| u | injection velocity | m/s |
| V_{ratio} | velocity ratio, $V_{ratio} = u_{\text{CH}_4} / u_{\text{O}_2}$ | - |
| ρ | density | kg/m^3 |
| Φ | equivalence ratio | - |

REFERENCES

- [1] A. Götz, C. Mäding, L. Brummer, D. Haeseler, *Application of non toxic propellants for future Advanced Launcher Vehicles.*, AIAA-2001-3546, 37th AIAA/ASME/SAE/ASEE Conference, July 2001
- [2] F. Cuoco, B. Yang, M. Oswald, *Experimental Investigation of LOx/H₂ and LOx/CH₄ Sprays and Flames*, ISTS 2004-a-04, 24th International Symposium on Space Technology and Science, Japan, June 2004
- [3] B. Yang, F. Cuoco, M. Oswald, *Atomization and Flames in LOX/H₂ and LOX/CH₄ Spray Combustion*, Journal of Propulsion and Power, Vol.23, No.4, July-August 2007
- [4] S.Candel, M.Juniper, G.Singla, P. Scoufflaire, C. Rolon, *Structure and dynamics of cryogenic flames at supercritical pressure*, Combustion Science and Technique, 178 161 192, 2006
- [5] G. Singla, P. Scoufflaire, C. Rolon, S. Candel, *Transcritical oxygen/transcritical or supercritical methane combustion*, Proceedings of the combustion institute, 30 2921 2928, 2005
- [6] J.D. Moore, G. A. Risha, K K. Kuo, B. Zhang, R. Wehrman, *Stability of Methane/Oxygen Coaxial Diffusion Flame*, 39th AIAA/ASME/SAE/ASEE Conference, 2003
- [7] V. Schmidt, U. Wepler, O.J. Haidn, M. Oswald, *Characterization of the Primary Ignition Process of a coaxial GH₂/LOx Spray*, AIAA 2004-1167
- [8] V. Schmidt, D. Klimenko, O.J. Haidn, M. Oswald, *Experimental Investigation and Modelling of Ignition Transient of a Coaxial H₂/O₂ Injector*, 5th International Symposium on Liquid Space Propulsion, Oct. 28-30 2003
- [9] G. Lacaze, B. Cuenot, T. Poinot, *LES of Laser Ignition in a micro-combustor*, CERFACS Internal Report
- [10] F. Cuoco, B. Yang, C. Bruno, O.J. Haidn, M. Oswald, *Experimental investigation on LOx/CH₄ Ignition*, AIAA 2004-4005, 40th AIAA Joint Propulsion Conference, July 11-14 2004, Florida
- [11] J.L. Beduneau, B. Kim, L. Zimmer, Y. Ikeda, *Measurements of minimum energy in premixed laminar methane/air flow by using laser induced spark*, Comb. And Flame 132(2003) 653-665